Uniplanar Power Dividers Using Coupled CPW and Asymmetrical CPS for MIC's and MMIC's

Lu Fan, *Member, IEEE* and Kai Chang, *Fellow, IEEE*

Abstract— **Uniplanar coplanar waveguide (CPW), coplanar strip (CPS), and slotline on dielectric substrates have many applications in microwave integrated circuit (MIC) and monolithic microwave/millimeter wave integrated circuit (MMIC) designs. New power dividers using one-section and two-section coupled CPW have been developed. These circuits provide substantially improved performance over a wider bandwidth than conventional microstrip power dividers. Measured results show that the one-section CPW power divider has greater than 20-dB isolation, less than 0.3-dB insertion loss, a 0.2-dB power dividing imbalance, and a 2° phase imbalance over a bandwidth of more than 30% centered at 3 GHz. The two-section CPW power divider has greater than 24-dB isolation, less than 0.5-dB insertion loss, a 0.1-dB power dividing imbalance, and a 1.6° phase imbalance over a bandwidth of more than 66% centered at 3 GHz. Experimental results agree well with calculated ones. In-phase and 180° out-of-phase power dividers constructed by the circuit configuration method are described in this paper. The even-odd mode excited method is used to analyze the power dividers. Also two other power dividers using asymmetrical coplanar strip (ACPS) have been developed with good performance. A 180° out-of-phase power divider is demonstrated with an amplitude imbalance of 0.4 dB and a phase difference of 180° ± 1° over a wide bandwidth.**

I. Introduction

THE development of high-performance and low-cost microwave devices and components is required for new wireless communication systems. Power dividers are fundamental and important components widely used in various microwave integrated circuit (MIC) applications such as balanced mixers, balanced amplifiers, phase shifters, and feed networks in antenna arrays. Over the last several decades, many designs, optimizations and theoretical developments have progressed on this subject [1]–[6]. The Wilkinson power divider, a popular two-way power divider/combiner, is a well-known example [7]. A power divider using coupled microstrip-slot lines was reported by Ogawa *et al.* [8] in 1985. However, this double-sided circuit configuration is not suitable for the monolithic microwave/millimeter wave integrated circuit (MMIC) implementation because it uses the back side of the substrate. Most previous work is based on microstrip structures because microstrip is the most mature and widely used transmission line.

Microstrip lines have been used as the main transmission lines in many MIC designs so far because the characteristics of microstrip lines are well known and a number of discontinuity problems have been analyzed. However, some shortcomings of microstrip include sensitivity to substrate thickness, difficulty in inserting shunt solid-state devices and the requirement of high impedance lines for dc biasing. In recent years, uniplanar transmission lines such as coplanar waveguide (CPW), coplanar strip (CPS), and slotline shown in Fig. 1(a) have become competitive alternatives to microstrip in many applications (including both microwave hybrid and monolithic technologies). These transmission lines have advantages of small dispersion, simple realization of short circuited ends, easy integration with lumped elements and active components, and no need for via holes. These characteristics make CPW, CPS, and slotline important in MIC and MMIC designs. Many attractive components using uniplanar structures have been reported [9]–[16]. Fig. 1(b) shows asymmetric uniplanar structures (ACPW [17], asymmetrical coplanar strip (ACPS) [18], and asymmetric slotline) which have been used as transmission lines in developing microwave components such as mixers [19], and attenuators [20].

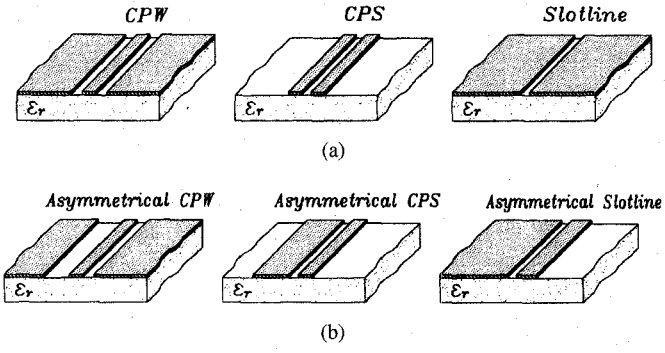

Fig. 1. Various uniplanar transmission lines. (a) Common CPW, CPS, and slotline and (b) asymmetrical CPW, CPS, and slotline.

In order to further extend uniplanar techniques to MIC and MMIC applications, additional uniplanar components are required. This paper presents new uniplanar power divider components that have characteristics similar to those of microstrip circuits with the advantages of a uniplanar structure and better performance. The general circuit configurations, equivalent circuits and design formulas for the uniplanar power dividers are described in Section II. Section III presents the construction and performance of the one-section and two-section in-phase coupled CPW power dividers. In addition, two ACPS Wilkinson power dividers with in-phase or 180° out-of-phase output ports are illustrated in Section IV. The circuit analyzes for the power dividers are based on simple transmission line models using the method of even-mode and

Manuscript received March 28, 1996. This work was supported in part by the Army Research Office.

The authors are with the Department of Electrical Engineering, Texas A&M University, College Station, TX 77843-3128 USA.

Publisher Item Identifier S 0018-9480(96)08516-X.

0018–9480/96$05.00 © 1996 IEEE

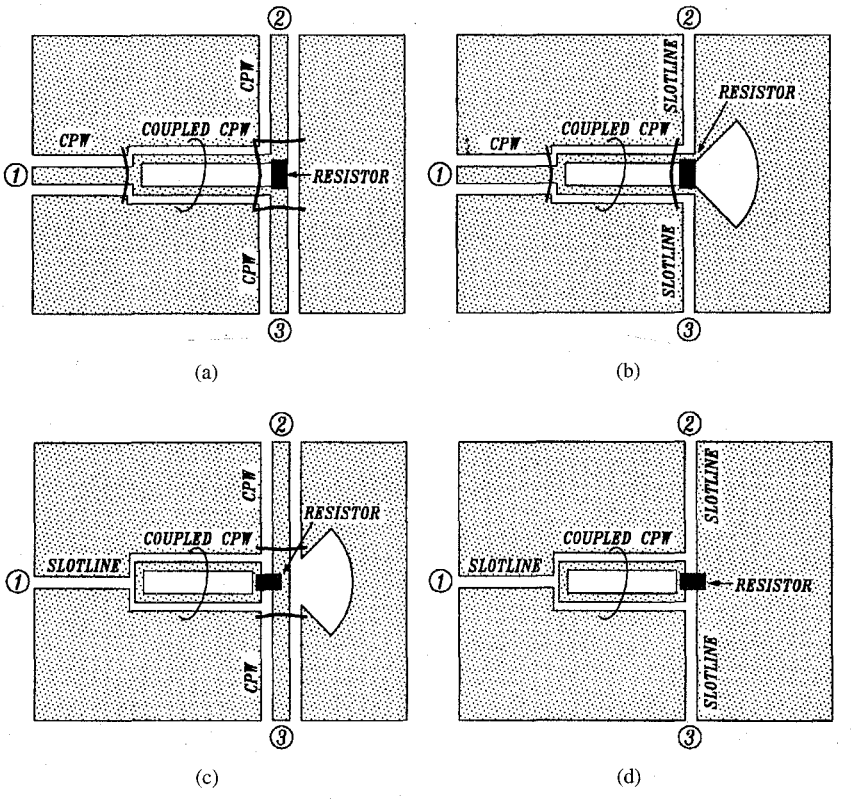

Fig. 2. Configurations of uniplanar power dividers. The power dividers (a) with CPW input/output arms and (b) with CPW input and slotline output arms are in-phase power dividers. The power dividers (c) with slotline input and CPW output arms and (d) with slotline input/output arms are 180° out-of-phase power dividers.

odd-mode. The simulations of the circuits have been performed using Libra and Sonnet and the measured results agree very well with the theoretical predictions.

II. Circuit Configurations and Design of Uniplanar Power Dividers

First, this section describes circuit configurations for uniplanar two-way coupled CPW power dividers. Then, the multisection equivalent circuit of the in-phase power dividers is shown and the design formulas for one-section and two-section circuits are given.

A. Circuit Configurations

Fig. 2 shows the physical configurations of the uniplanar power dividers. The circuits consist of a quarter-wavelength section of coupled CPW, a mini size chip resistor, and a CPW or slotline input and two CPW or slotline outputs. The output types are very flexible depending on circuit application requirements. In terms of the phase between output ports, power dividers can be classified into in-phase and out-of-phase dividing types. Fig. 2(a) and (b) show in-phase types with CPW and slotline outputs, respectively. Fig. 2(c) and (d) show out-of-phase types with CPW and slotline outputs, respectively. Therefore, the power dividers formed by coupled CPW can be applied to various types of circuit configurations with uniplanar advantages.

Fig. 3 shows schematic explanation of the circuit behavior for the in-phase and out-of-phase types, respectively. The arrows in the figure indicate the direction of the electric field in the CPW, coupled CPW, and slotlines. In Fig. 3(a), the input signal fed to port 1 propagates through the CPW, and is then converted to the even mode of the coupled CPW. After propagating through the coupled CPW, it is divided into two components that both arrive in-phase at ports 2 and 3. In Fig. 3(b), the input signal fed to port 1 propagates through the CPW and is then converted to the odd mode of the coupled CPW (i.e., coupled slotline mode). After propagating through the coupled CPW, it is divided into two components that arrive at ports 2 and 3 with a 180° phase difference. The 180° phase difference is due to the input slotline T-junction.

B. Design Formulas

Fig. 4(a) and (b) show multisection uniplanar power dividers that are generalizations of the circuits in Fig. 2(a) and (d). The in-phase type circuit in Fig. 4(a) is symmetric with respect to port 1 and analyzed by even-mode and odd-mode excitations of ports 2 and 3 with a load Z_0 connected to port 1 [3]. Fig. 5 shows the equivalent circuits when ports 2 and 3 are excited by the even and odd modes. In Fig. 5, the R_i $(i = 1 \sim n)$ are isolation resistors in the ith sections between ports 2 and 3, and θ_{ei}, Z_{ei} and θ_{oi}, Z_{oi} $(i = 1 \sim n)$ are the electrical lengths and characteristic impedances in the ith sections of the even mode and the odd mode of the coupled CPW, respectively.

In Fig. 5, Γ_e and Γ_o are the voltage reflection coefficients of the circuits in Fig. 4(a). The voltage reflection coefficients Γ_1, Γ_2, and Γ_3 at ports 1, 2, and 3 of the complete power

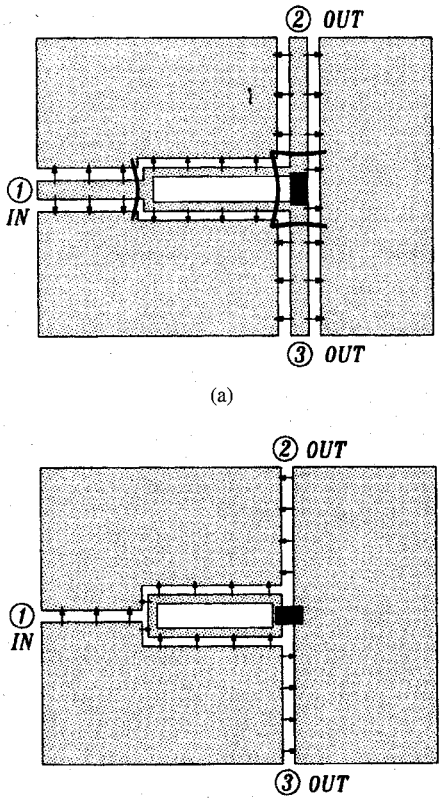

Fig. 3. Schematic expression of the electric field distributions for (a) in-phase power divider in Fig. 2(a) and (b) 180° out-of-phase power divider in Fig. 2(d).

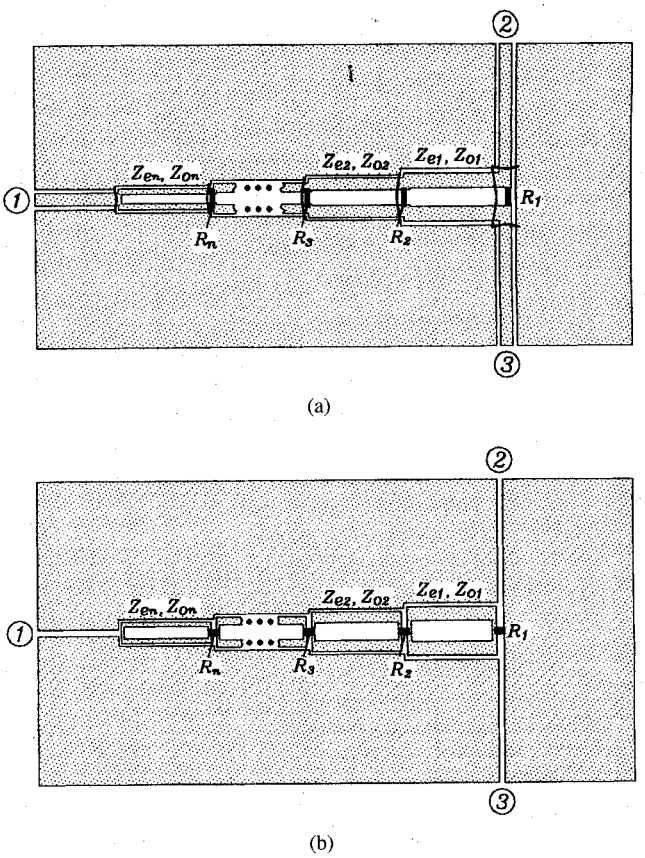

Fig. 4. Multisection uniplanar (a) in-phase and (b) 180° out-of-phase power dividers.

divider in Fig. 4(a), and the voltage transmission coefficients T_{12}, T_{13}, and T_{23} between those ports are given as follows [3]:

$$|\Gamma_1| = |\Gamma_e| \tag{1a}$$

$$\Gamma_2 = \Gamma_3 = \tfrac{1}{2}(\Gamma_e + \Gamma_o) \tag{1b}$$

$$|T_{12}| = |T_{13}| = \frac{1}{\sqrt{2}}(1 - |\Gamma_e|^2)^{1/2} \tag{1c}$$

$$T_{23} = \tfrac{1}{2}(\Gamma_e - \Gamma_o). \tag{1d}$$

Thus, all reflection and transmission coefficients of the general three-port symmetrical circuit in Fig. 4(a) can be calculated by (1a)–(1d). To find the even and odd mode characteristic impedances and resistors, assume the following conditions: 1) θ_{ei} and θ_{oi} $(i = 1 \sim n)$ are equal to 90°; 2) the Z_{ei} $(i = 1 \sim n)$ are designed to yield an optimum stepped-transformer response (i.e., equal-ripple behavior in a specified bandwidth of f_1 and f_2) between terminal impedances Z_0 and $2Z_0$; 3) the R_i $(i = 1 \sim n)$ are calculated from the impedance matching condition of the circuit in Fig. 5(b). Then the design formulas are derived. The formulas for one-section and a two-section power dividers are given below. All characteristic impedances and resistors are normalized by the load impedance Z_0.

For one-section power divider

$$Z_{e1} = \sqrt{2} \tag{2}$$

$$R_1 = 2. \tag{3}$$

For two-section power divider

$$Z_{e1} = \left[\left(2 + \frac{1}{4\tan^4\phi}\right)^{1/2} + \frac{1}{2\tan^2\phi}\right]^{1/2} \tag{4a}$$

$$Z_{e2} = \frac{2}{Z_{e1}} \tag{4b}$$

$$R_2 = \frac{2\,Z_{o1}\,Z_{o2}}{(Z_{o1} + Z_{o2})^{1/2}(Z_{o2} - Z_{o1}\cot^2\phi)^{1/2}} \tag{5a}$$

$$R_1 = \frac{2R_2(Z_{o1} + Z_{o2})}{R_2(Z_{o1} + Z_{o2}) - 2Z_{o2}} \tag{5b}$$

where

$$\phi = \frac{\pi}{4}\left[1 - \frac{1}{\sqrt{2}}\left(\frac{\frac{f_2}{f_1} - 1}{\frac{f_2}{f_1} + 1}\right)\right] \tag{6}$$

$$\text{Bandwidth} = f_2 - f_1. \tag{7}$$

Although the design formulas have been derived for the in-phase type of power divider, these formulas can also be used for designing the out-of-phase power divider by exchanging the odd mode characteristic impedance for the even mode one and taking their reciprocals.

III. Uniplanar Coupled CPW Power Dividers

According to the above design principal, one-section and two-section coupled CPW two-way power dividers have been

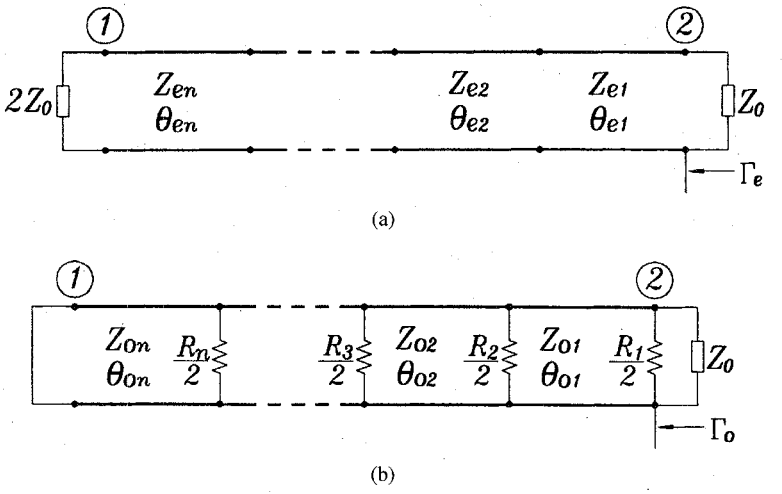

Fig. 5. Equivalent circuits for the in-phase power divider in Fig. 4(a). (a) Even mode excited circuit and (b) odd mode excited circuit.

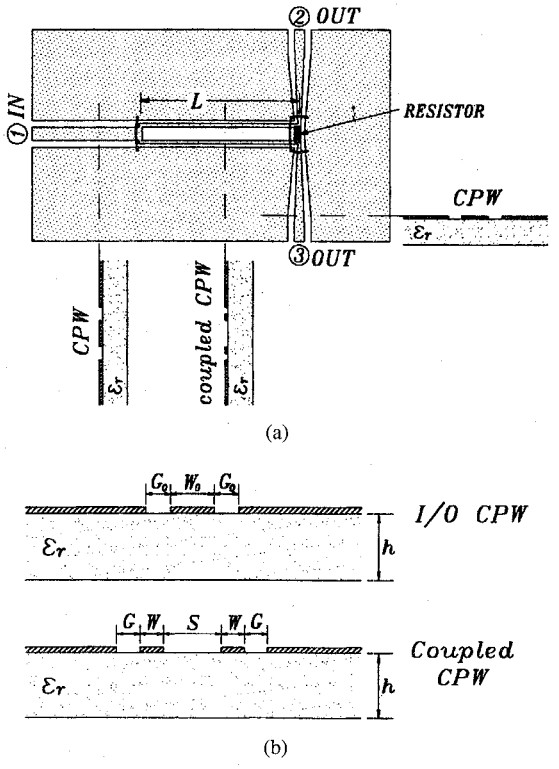

Fig. 6. One-section in-phase coupled CPW power divider. (a) Circuit configuration, (b) cross section views of the CPW and coupled CPW, and (c) equivalent transmission line model of the one-section power divider.

designed at the center frequency of 3 GHz to confirm the design.

A. One-Section Coupled CPW Power Divider

Fig. 6 shows the physical configuration of the one-section coupled CPW power divider. The circuit consists of a CPW input line, a quarter-wavelength coupled CPW, a mini size chip resistor, and two CPW outputs (or two slotline outputs) as shown in Fig. 6(a). The equivalent transmission line model of the power divider is shown in Fig. 6(c). The parallel transmission lines represent the coupled CPW operating in even and odd modes. In Fig. 6(c), R is an isolation resistor between ports 2 and 3, and θ_e, Z_e and θ_o, Z_o are the electrical lengths and characteristic impedances of the even mode and odd mode of the coupled CPW, respectively. If θ_e and θ_o are equal to 90°, from (2) and (3), then $Z_e = \sqrt{2}Z_0$ and $R = 2Z_0$ are obtained. Although there is no restriction for Z_o, it should be given a value easy to implement in practical circuits. Actually, the operation bandwidth of the circuit depends on the ratio of Z_e and $Z_o (r = Z_e/Z_o)$. When r is equal to 1 $(Z_e = Z_o)$, the power divider is composed of non coupled lines with the widest bandwidth. The larger that r is, the narrower the bandwidth is. Therefore, choosing the value of Z_o close to Z_e is necessary.

TABLE I
THE GEOMETRICAL PARAMETERS OF ONE-SECTION COUPLED CPW POWER DIVIDER AS SHOWN IN FIG. 6 (ALL DIMENSIONS ARE IN MM)

I/O CPW		Coupled CPW			
W_0	G_0	W	G	S	L
0.62	0.33	0.17	0.1	0.8	10.74

The one-section coupled CPW power divider was fabricated on an RT/Duriod 6010 substrate (relative dielectric constant $\epsilon_r = 10.8$, substrate thickness $h = 1.524$ mm, metal thickness $t = 18\,\mu$m). The characteristic impedances of the input/output CPW's were chosen as $Z_0 = 50\,\Omega$, resulting in the characteristic impedance $Z_e = 71\,\Omega$ and isolation resistance $R = 100\,\Omega$. From these known values, simulation and synthesis for the practical circuit were performed using Libra. The relevant geometrical parameters are listed in Table I. It is important to note that the use of air bridges at the circuit's discontinuities prevents the coupled slotline mode from propagating on the CPW lines. The measurements were made on an HP-8510 network analyzer using standard SMA connectors. The insertion loss includes two coaxial-to-CPW transitions and 30-mm-long input/output CPW lines.

The practical circuit shown in Fig. 6(a) was tested from 1–5 GHz. Fig. 7(a) and (b) show the power divider's measured and calculated insertion loss, return loss and isolation. Over a 30% bandwidth centered at 3 GHz, the insertion loss is less than

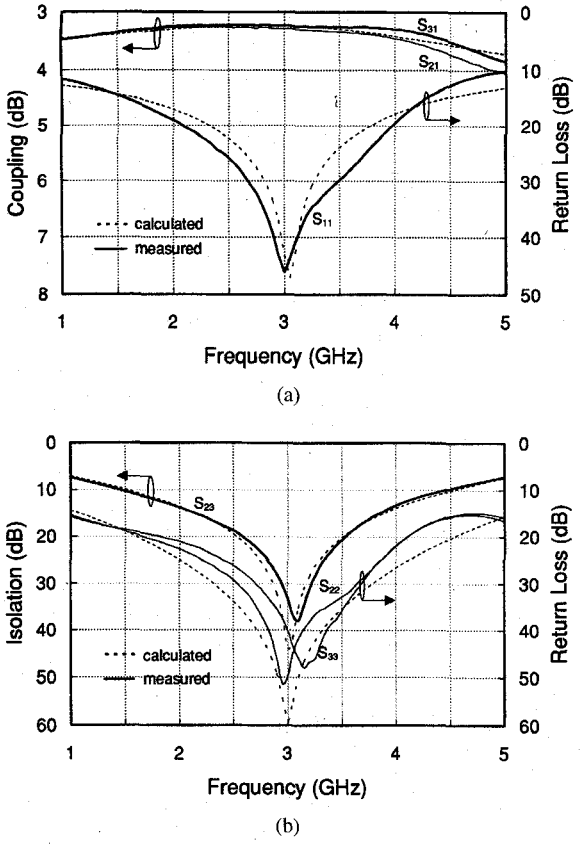

Fig. 7. Measured and calculated frequency responses of the one-section coupled CPW power divider shown in Fig. 6(a) at the center frequency of 3 GHz. (a) Coupling of 1-2 and 1-3 and 1-port's return loss. (b) 2-port's and 3-port's return losses and isolation between ports 2 and 3.

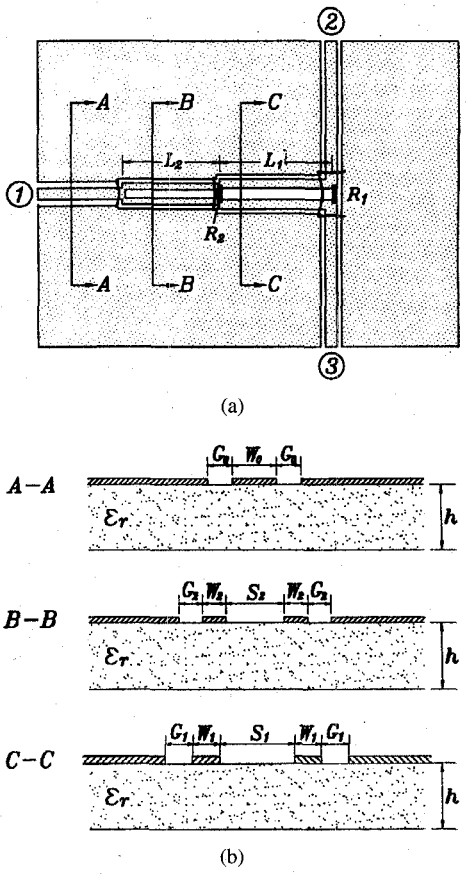

Fig. 8. Two-section in-phase coupled CPW power divider. (a) Circuit configuration, (b) cross section views of the CPW and coupled CPW's, and (c) equivalent transmission line model.

3.3 dB (3 dB for ideal coupling) and the input return loss is greater than 26 dB as shown in Fig. 7(a). The isolation ($|S_{32}|$) between the two output ports is greater than 20 dB and the return losses of ports 2 and 3 are greater than 27 dB, as shown in Fig. 7(b). Fig. 7(a) and (b) also indicate that the experimental results agree very well with the calculations.

B. Two-Section Coupled CPW Power Divider

The multisection approach can be used to extend the bandwidth of power dividers [3]. A two-section in-phase coupled CPW power divider was also designed and fabricated. Fig. 8(a) shows the circuit configuration of the power divider that consists of a CPW input line, two quarter-wavelength coupled CPW sections, two mini-size chip resistors, and two CPW outputs. Fig. 8(b) shows the cross sections at three locations along the power divider. The equivalent transmission line model of the power divider is shown in Fig. 8(c). Two pairs of parallel transmission lines represent the coupled CPW operating in even mode and odd mode. In Fig. 8(c), R_1 and R_2 are isolation resistors between ports 2 and 3, and θ_{e1}, θ_{e2}, Z_{e1}, Z_{e2} and θ_{o1}, θ_{o2}, Z_{o1}, Z_{o2} are the electrical lengths and characteristic impedances of the even mode and odd mode of the coupled CPW sections, respectively. According to (4)–(6), the characteristic impedances and resistors of the circuit were calculated for $Z_0 = 50\,\Omega$ over a bandwidth from 2–4 GHz ($f_2/f_1 = 2$). The isolation resistances are $R_1 = 651\,\Omega$ and $R_2 = 62.5\,\Omega$, and the characteristic impedances are $Z_{e1} = 61\,\Omega$ and $Z_{e2} = 82\,\Omega$. From these known values, synthesis and optimizing for the dimensions of the circuit were performed using Libra. The relevant geometrical parameters of the two-section power divider are listed in Table II.

TABLE II
THE GEOMETRICAL PARAMETERS OF TWO-SECTION COUPLED CPW POWER DIVIDER AS SHOWN IN FIG. 8 (ALL DIMENSIONS ARE IN MM)

I/O CPW		Coupled CPW							
W_0	G_0	W_1	G_1	S_1	L_1	W_2	G_2	S_2	L_2
0.62	0.33	0.52	0.12	1.2	10.8	0.17	0.18	0.8	10.7

Similarly, the two-section power divider was fabricated on an RT/Duriod 6010 substrate ($\epsilon_r = 10.8$, $h = 1.524$ mm, $t = 18\,\mu$m). Adding air bridges at the circuit's discontinuities is important to prevent the coupled slotline mode from propagating on the CPW lines. During testing, the circuit was connected to an HP-8510 network analyzer using standard SMA connectors. The insertion loss includes the loss of two coaxial-to-CPW transitions and 38 mm long input/output CPW lines which were not calibrated out. The experimental data are shown in Fig. 9. Over a 66% bandwidth from 2–4 GHz, Fig. 9(a) shows that the insertion loss ($|S_{21}|$ or $|S_{31}|$) is less than 3.5 dB (3 dB for ideal coupling) and the isolation ($|S_{32}|$) is greater than 24 dB. The input return loss ($|S_{11}|$) is greater

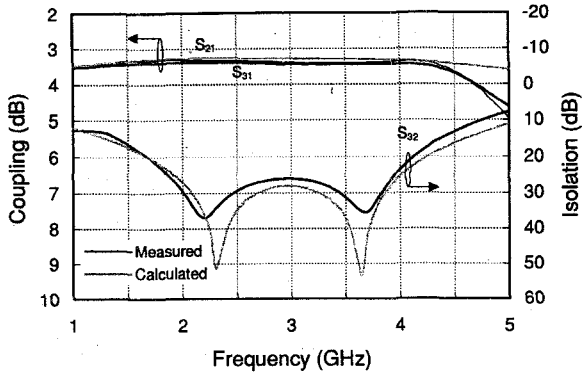

(a)

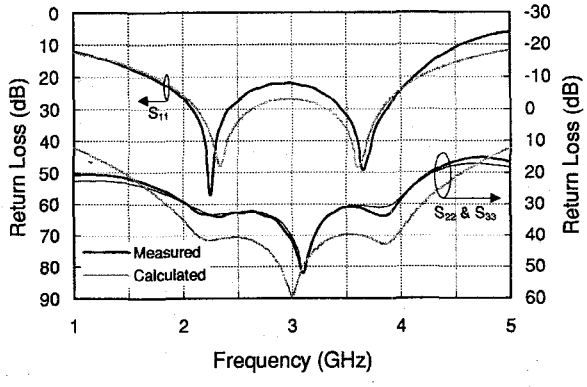

(b)

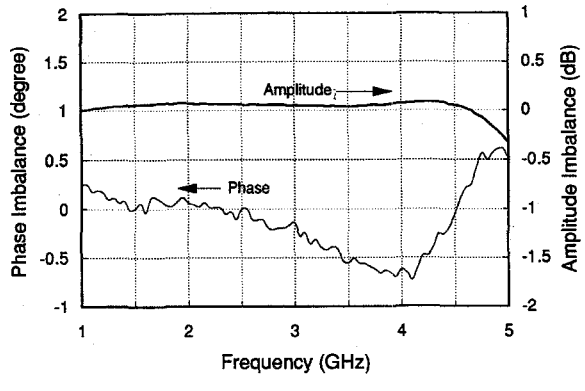

(c)

Fig. 9. Measured and calculated frequency responses of the two-section coupled CPW power divider shown in Fig. 8(a) at the center frequency of 3 GHz. (a) Coupling of 1-2 and 1-3 and isolation between ports 2 and 3. (b) 1-port's, 2-port's, and 3-port's return losses. (c) Amplitude and phase imbalances between ports 2 and 3.

than 21.5 dB and the return losses of ports 2 and 3 ($|S_{22}|$ and $|S_{33}|$) are greater than 29 dB as shown in Fig. 9(b). Excellent output amplitude imbalance (0.1 dB) and phase imbalance (1.6°) were achieved as shown in Fig. 9(c). Fig. 9(a) and (b) also indicates that the experimental results agree very well with the simulations. Obviously, the bandwidth of the two-section power divider is much greater than that of the one-section circuit.

As a result, the design of one- and two-section uniplanar power dividers using coupled CPW has been confirmed by measurements. The circuits exhibit performance over a wide bandwidth as compared to conventional microstrip power dividers.

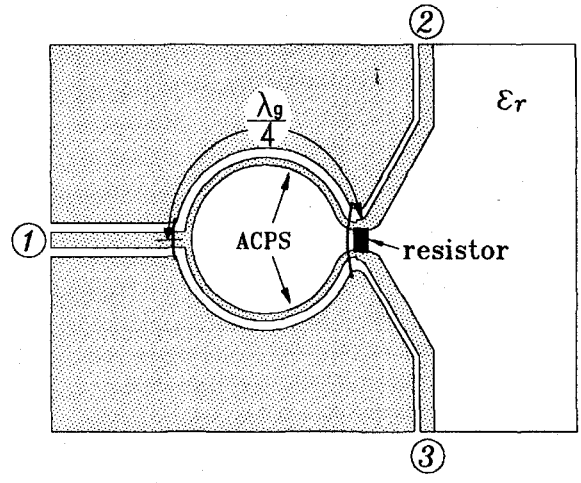

(a)

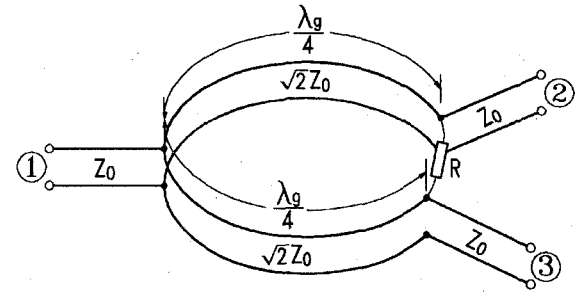

(b)

Fig. 10. Asymmetrical coplanar strip (ACPS) in-phase power divider. (a) Circuit configuration and (b) equivalent transmission line model.

IV. Uniplanar ACPS Wilkinson Power Dividers

Recently, asymmetrical uniplanar transmission lines [17] and [18] have been used as alternatives to symmetrical ones because of the additional flexibility offered by the asymmetric configuration in the design of MIC's. The applications of ACPW to mixers [19] and attenuators [20] have been reported by D. Jaisson. To further extend the asymmetric uniplanar techniques to MIC and MMIC applications, additional uniplanar components are required. This section describes two other uniplanar power using ACPS with in-phase and 180° out-of-phase output ports

A. In-Phase ACPS Power Divider

Fig. 10(a) shows the circuit layout of the in-phase ACPS Wilkinson power divider that is realized on one side of the substrate using CPW and ACPS transmission lines. The circuit consists of a CPW–ACPS tee junction, a pair of ACPS arms, a mini size chip resistor, and two ACPS outputs. Unlike the dividers described in Section III, the two arms of the divider in Fig. 10(a) are separated without coupling. The equivalent transmission line model of the power divider is shown in Fig. 10(b).

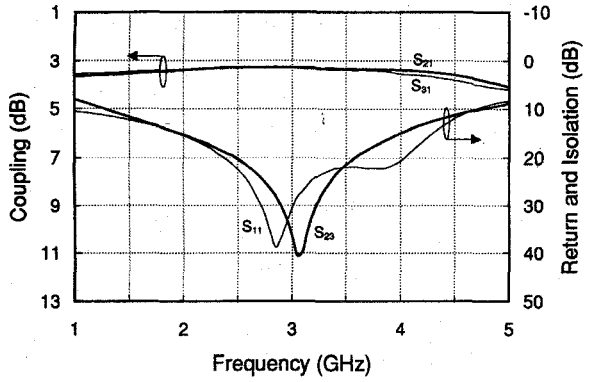

Fig. 11. Experimental performance of the ACPS in-phase power divider.

As in the divider's case in Section III, the ACPS power divider was fabricated on a 1.524 mm-thick RT/Duriod 6010 ($\epsilon_r = 10.8$) substrate. The center frequency is 3.0 GHz. The dimensions of the circuit are given as follows:

1) *CPW Feed Lines:* $Z_0 = 50\,\Omega$ (center strip width $W = 0.62$ mm, gap size $G = 0.33$ mm);
2) *ACPS Output Lines:* $Z_0 = 50\,\Omega$ (strip width $S_{acps} = 0.7$ mm, gap size $G_{acps} = 0.1$ mm);
3) *ACPS Arm's Lines:* $\sqrt{2}Z_0 = 71\,\Omega$ (strip width $S_{\rm acps} = 0.4$ mm, gap size $G_{\rm acps} = 0.3$ mm);
4) *ACPS Arm's Length:* $\lambda_g/4 = 9.54$ mm;
5) *Isolation Resistor:* $R = 100\,\Omega$.

To find the dimensions of the ACPS lines in the circuit, Sonnet software was used to perform the syntheses. Bonding wires were placed at the power divider's CPW–ACPS tee junction to enforce even mode propagation on the ACPS lines. The tests were made on an HP-8510 network analyzer using standard SMA connectors from 1–5 GHz. Fig. 11 shows the power divider's measured frequency responses of coupling, isolation, input return loss, amplitude imbalance and phase imbalance. Over a 30% bandwidth centered at 3 GHz, the measured results show that the coupling of the power from port 1 to ports 2 and 3 are 3.34 dB and 3.37 dB, respectively. The isolation between ports 2 and 3 is greater than 21 dB, and the input return loss is more than 22 dB both over a frequency range from 2.5–3.5 GHz. The amplitude difference and phase difference between ports 2 and 3 are excellent over a broad bandwidth. This ACPS power divider's characteristics are similar to those of the one-section coupled CPW power divider.

B. 180° Out-of-Phase ACPS Power Divider

As mentioned in Section II, power dividers are divided into in-phase and out-of-phase types. To confirm the basic behavior of the out-of-phase power divider with a uniplanar structure, this section describes a 180° out-of-phase ACPS Wilkinson power divider. The circuit consists of a slotline input line, a slotline-ACPS T-junction, a ACPS ring severing as two ACPS arms, a chip resistor, and two ACPS (CPW, slotline) outputs as shown in Fig. 12(a). It is important to point out here that the two arms of the divider are separated without coupling. The slotline-ACPS T-junction of

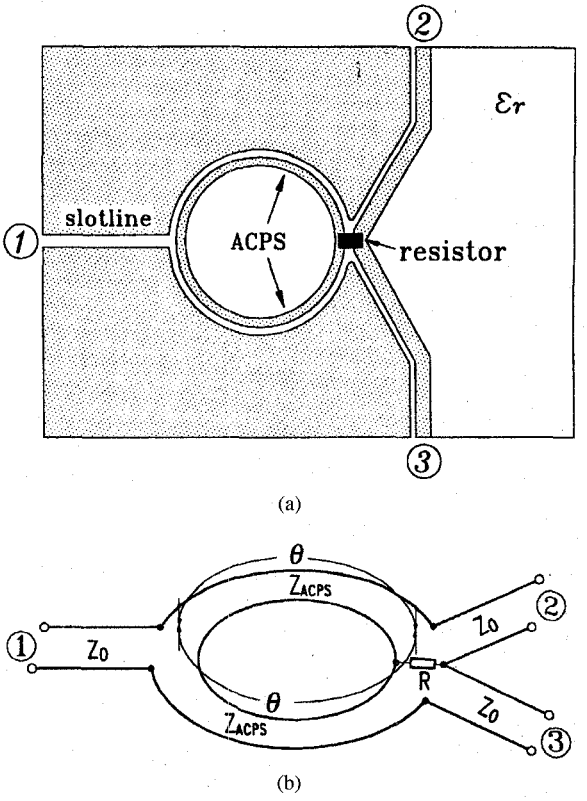

(a)

(b)

Fig. 12. Asymmetrical coplanar strip (ACPS) 180° out-of-phase power divider. (a) Circuit configuration and (b) equivalent transmission line model.

the divider is used as a phase inverter. Fig. 12(b) shows the equivalent transmission line model of the divider. The fundamental behavior of the divider can easily be understood by examining the equivalent circuit. The input signal is fed to port 1 and then divided into two components with a 180° phase difference (made by the slotline-ACPS reverse-phase T-junction) to the ACPS arms. After propagating through the ACPS arms, the two components arrive out-of-phase at ports 2 and 3.

Similar to the approach used in Section II-B, the symmetrical circuit in Fig. 12(b) is also analyzed by even-mode and odd-mode excitations of ports 2 and 3 with a load Z_0 connected to port 1. Fig. 13 shows the equivalent circuits when ports 2 and 3 are excited by the even and odd modes. In Fig. 13, R is an isolation resistor, and θ and $Z_{\rm ACPS}$ are the electrical length and characteristic impedance of the ACPS, respectively. By choosing θ to be equal to $90°, Z_{\rm ACPS} = Z_0/\sqrt{2}$, and $R = Z_0/2$ are obtained. These results are just equal to the reciprocals of (2) and (3). Actually, this is a special case of the one-section coupled CPW divider without coupling ($Z_e = Z_o$).

The 180° out-of-phase ACPS divider was designed, fabricated and tested with the same procedure used in the case of the in-phase ACPS divider. Note two points here: 1) The characteristic impedances of the input slotline and output ACPS lines were chosen as $Z_0 = 100\,\Omega$, resulting in the characteristic impedance of the two ACPS arms $Z_{\rm ACPS} = 71\,\Omega$ and the isolation resistance $R = 50\,\Omega$. If a $Z_0 = 50\,\Omega$ is chosen, the $Z_{\rm ACPS}$ is $35\,\Omega$ which is very difficult to

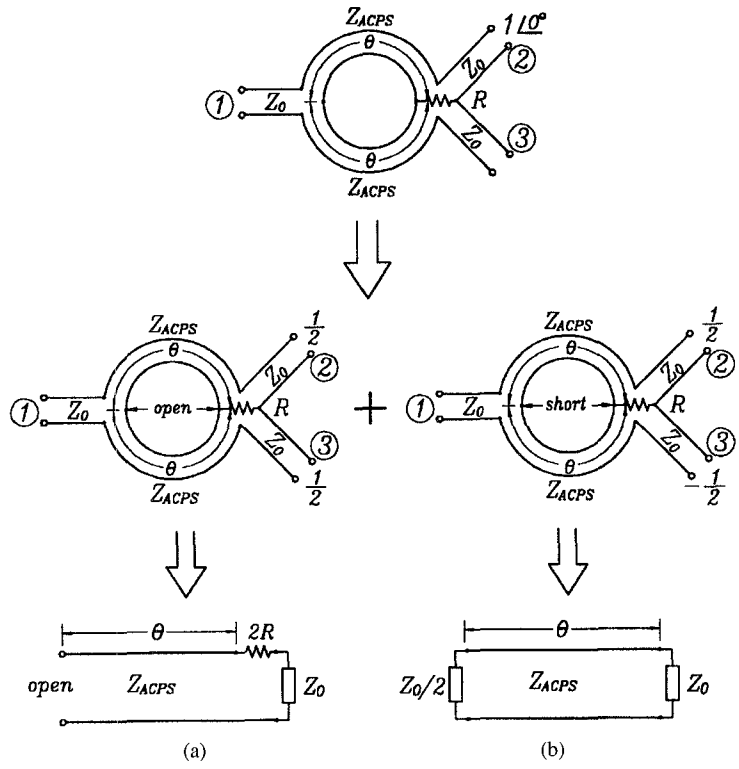

Fig. 13. Equivalent circuits of the ACPS 180° out-of-phase power divider for (a) in-phase and (b) out-of-phase excitations.

TABLE III
SUMMARY OF MEASURED PERFORMANCES OF THE COUPLED CPW AND ACPS POWER DIVIDERS

Type of Power Divider	Operation Bandwidth* (%)	Insertion Loss (S_{21}, S_{31}) (dB)	Isolation (S_{32}) (dB)	Return Loss (dB) Input (S_{11})	Return Loss (dB) Output (S_{22}, S_{33})	Amplitude Imbalance ($\|S_{21}\|/\|S_{31}\|$) (dB)	Phase Difference ($\angle S_{21} - \angle S_{31}$) (degree)
One-section Coupled CPW	> 30	< 0.3	> 20	> 26	> 27	< 0.2	0 ± 1
Two-section Coupled CPW	> 66	< 0.5	> 24	> 21.5	> 29	< 0.1	0 ± 0.8
ACPS In-phase	> 30	< 0.4	> 21	> 22	> 25	< 0.2	0 ± 1
ACPS Out-of-phase	> 13	< 0.8	> 20.5	> 20	> 21	< 0.3	180 ± 1

* Center frequency is at 3 GHz. All the specifications in the table are over the corresponding bandwidth.

implement using ACPS. 2) Bonding wires are not needed in this case.

Fig. 14 shows the out-of-phase divider's measured performances which are also summarized in Table III. Although the insertion loss, return loss and isolation of the divider are over a narrow bandwidth of 13% compared to the in-phase dividers, the divider's amplitude difference and phase difference between ports 2 and 3 are excellent over a broad bandwidth because the phase reversal of the slotline-ACPS T-junction is frequency independent.

V. CONCLUSION

The design procedure and results of newly developed uniplanar power dividers using coupled CPW and ACPS were described. The measured performances of the power dividers are summarized in Table III. Although all results are given for the band of 1–5 GHz, the circuit designs can be scaled up to millimeter-wave frequencies with the effects of discontinuities included. From the experimental results, the conclusions are as follows.

1) The one-section coupled CPW and ACPS in-phase power dividers have greater than 20-dB isolation and return loss, less than 0.3-dB insertion loss, a 0.2 dB amplitude imbalance and a 2° phase imbalance over a bandwidth of more than 30% centered at 3 GHz.
2) The two-section in-phase coupled CPW power divider gives better performance than the one-section power dividers over a wide bandwidth of more than 66%,

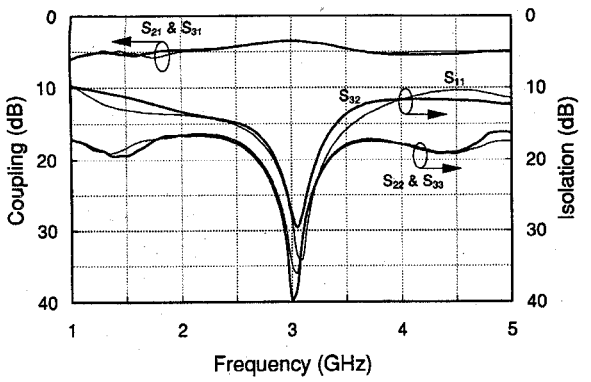

(a)

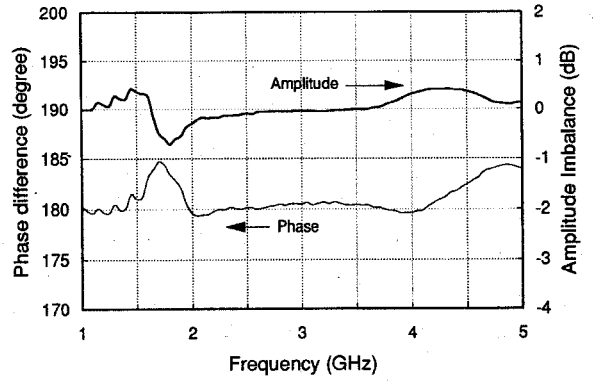

(b)

Fig. 14. Experimental performance of the 180° out-of-phase ACPS power divider. (a) Coupling, return loss, and isolation; (b) amplitude imbalance and phase difference.

but the insertion loss is slightly higher. The use of the multisection technique can increase the bandwidth of the power dividers.

3) The 180° out-of-phase ACPS power divider has a good amplitude imbalance and phase difference over a wide bandwidth, but insertion loss, isolation and return loss are over a narrow bandwidth as compared to the above in-phase power dividers.

In all, these power dividers demonstrated good performance over a wider bandwidth than is possible with conventional microstrip power dividers. With its advantages of a compact, simple, uniplanar structure and ease of integration with solid-state devices, these uniplanar power dividers will be useful in many applications for MIC's and MMIC's.

REFERENCES

[1] E. J. Wilkinson, "An N-way hybrid power divider," *IRE Trans. Microwave Theory Tech.*, vol. MTT-8, pp. 116–118, Jan. 1960.
[2] L. I. Parad and R. L. Moynihan, "Split-tee power divider," *IEEE Trans. Microwave Theory Tech.*, vol. MTT-13, pp. 91–95, Jan. 1965.
[3] S. B. Cohn, "A class of broadband three-port TEM-mode hybrids," *IEEE Trans. Microwave Theory Tech.*, vol. MTT-16, pp. 110–116, Feb. 1968.
[4] R. B. Ekinge, "A new method of synthesizing matched broad-band TEM mode three ports," *IEEE Trans. Microwave Theory Tech.*, vol. MTT-19, pp. 81–88, Jan. 1971.
[5] A. M. Saleh, "Planar electrically symmetric N-way hybrid power dividers/combiners," *IEEE Trans. Microwave Theory Tech.*, vol. MTT-28, pp. 555–563, June 1980.
[6] D. Kother, B. Hopf, T. Sporkmann, and I. Wolff, "MMIC Wilkinson couplers for frequencies up to 110 GHz," in *IEEE MTT-S Int. Microwave Symp. Dig.*, 1995, pp. 663–666.
[7] S. Y. Liao, *Microwave Transistor Amplifiers Analysis and Design.* Englewood Cliffs, NJ: Prentice-Hall, 1984, p. 176.
[8] H. Ogawa, T. Hirota, and M. Aikawa, "New MIC power dividers using coupled microstrip-slot lines: Two-sided MIC power dividers," *IEEE Trans. Microwave Theory Tech.*, vol. MTT-33, pp. 1155–1164, Nov. 1985.
[9] M. Abdo Tuko and I. Wolff, "Novel 36 GHz GaAs frequency doublers using (M)MIC coplanar technology," in *IEEE MTT-S Int. Microwave Symp. Dig.*, 1992, pp. 1167–1170.
[10] D. Cahana, "A new coplanar waveguide/slotline double-balanced mixer," in *IEEE MTT-S Int. Microwave Symp. Dig.*, 1989, pp. 967–968.
[11] T. Tokumitsu, S. Hara, and M. Aikawa, "Very small ultra-wide-band MMIC magic-T and applications to combiners and dividers," *IEEE Trans. Microwave Theory Tech.*, vol. 37, pp. 1985–1990, Dec. 1989.
[12] C. H. Ho, L. Fan, and K. Chang, "Broad-band uniplanar hybrid-ring and branch-line couplers," *IEEE Trans. Microwave Theory Tech.*, vol. 41, pp. 2116–2125, Dec. 1993.
[13] D. I. Kim and Y. Naito, "Broad-band design of improved hybrid-ring 3-dB directional coupler," *IEEE Trans. Microwave Theory Tech.*, vol. MTT-30, pp. 2040–2046, Nov. 1982.
[14] C. H. Ho, L. Fan, and K. Chang, "New uniplanar coplanar waveguide hybrid-ring couplers and magic-Ts," *IEEE Trans. Microwave Theory Tech.*, vol. 42, pp. 2440–2448, Dec. 1994.
[15] Y. H. Shu, J. A. Navarro, and K. Chang, "Electronically switchable and tunable coplanar waveguide-slotline band-pass filter," *IEEE Trans. Microwave Theory Tech.*, vol. 39, pp. 548–554, Mar. 1991.
[16] L. Fan, C. H. Ho, S. Kanamaluru, and K. Chang, "Wide-band reduced-size uniplanar magic-T, hybrid-ring, and De Ronde's CPW-slot couplers," *IEEE Trans. Microwave Theory Tech.*, vol. 43, pp. 2749–2758, Dec. 1995.
[17] V. F. Hanna and D. Thebault, "Theoretical and experimental investigation of asymmetric coplanar waveguides," *IEEE Trans. Microwave Theory Tech.*, vol. MTT-32, pp. 1649–1651, Dec. 1984.
[18] I. Kneppo and J. Gotzman, "Basic parameters of non symmetrical coplanar lines," *IEEE Trans. Microwave Theory Tech.*, vol. MTT-25, p. 718, Aug. 1977.
[19] D. Jaisson, "A single-balanced mixer with a coplanar balun," *Microwave J.*, vol. 35, pp. 87–96, July 1992.
[20] ——, "A microwave-coplanar waveguide coupler for use with an attenuator," *Microwave J.*, vol. 38, pp. 120–130, Sept. 1995.

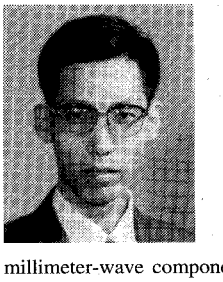

Lu Fan (M'96) received the B.S. degree in electrical engineering from Nanjing Institute of Technology (now the Southeast University), in Nanjing, China, in 1982.

From September 1982 to December 1990, he was with the Department of Radio Engineering of Nanjing Institute of Technology as a Teaching Assistant and Lecturer. In January 1991, he became a Research Associate in the Department of Electrical Engineering, Texas A&M University, College Station. His research interests include microwave and millimeter-wave components and active antennas.

Kai Chang (S'75–M'76–SM'85–F'91) received the B.S.E.E. degree from the National Taiwan University, Taipei, Taiwan, the M.S. degree from the State University of New York at Stony Brook, and Ph.D. degree from the University of Michigan, Ann Arbor, in 1970, 1972, and 1976, respectively.

From 1972 to 1976, he was with the Microwave Solid-State Circuits Group, Cooley Electronics Laboratory of the University of Michigan, as a Research Assistant. From 1976 to 1978, he was employed by Shared Applications, Inc., Ann Arbor, MI, where he worked in computer simulation of microwave circuits and microwave tubes. From 1978 to 1981, he was with the Electron Dynamics Division, Hughes Aircraft Company, Torrance, CA, where he was involved in the research and development of millimeter-wave, solid-state devices and circuits, power combiners, oscillators, and transmitters. From 1981 to 1985, he was with the TRW Electronics and Defense, Redondo Beach, CA, as a Section Head, developing state-of-the-art millimeter-wave integrated circuits and subsystems including mixers, VCO's, transmitters, amplifiers, modulators, up-converters, switches, multipliers, receivers, and transceivers. He joined the Electrical Engineering Department of Texas A&M University in August 1985 as an Associate Professor and was promoted to a Professor in 1988. In January 1990, he was appointed E-Systems Endowed Professor of Electrical Engineering. His current interests are in microwave and millimeter-wave devices and circuits, microwave integrated circuits, integrated antennas, wideband and active antennas, phased arrays, microwave power transmission, and microwave optical interactions. He has authored and coauthored several books, including, *Microwave Solid-State Circuits and Applications* (New York: Wiley, 1994), *Microwave Ring Circuits and Antennas* (New York: Wiley, 1996), and *Integrated Active Antennas and Spatial Power Combining* (John Wiley, 1996). He served as the editor of the four-volume, *Handbook of Microwave and Optical Components* (New York: Wiley, 1989, 1990). He is editor of the *Microwave and Optical Technology Letters* and the Wiley Book Series: *Microwave and Optical Engineering*. He has published more than 250 technical papers and several book chapters in the areas of microwave and millimeter-wave devices, circuits, and antennas.

Dr. Chang received the Special Achievement Award from TRW in 1984, the Halliburton Professor Award in 1988, the Distinguished Teaching Award in 1989, the Distinguished Research Award in 1992, and the TEES Fellow Award in 1996 from Texas A&M University.